

WAN: Watermarking Attack Network

Seung-Hun Nam^{*†}, Wonhyuk Ahn^{*}, In-Jae Yu, and Seung-Min Mun

Abstract—Multi-bit watermarking (MW) has been developed to improve robustness against signal processing operations and geometric distortions. To this end, benchmark tools that test robustness by applying simulated attacks on watermarked images are available. However, limitations in these general attacks exist since they cannot exploit specific characteristics of the targeted MW. In addition, these attacks are usually devised without consideration of visual quality, which rarely occurs in the real world. To address these limitations, we propose a watermarking attack network (WAN), a fully trainable watermarking benchmark tool that utilizes the weak points of the target MW and induces an inversion of the watermark bit, thereby considerably reducing the watermark extractability. To hinder the extraction of hidden information while ensuring high visual quality, we utilize a residual dense blocks-based architecture specialized in local and global feature learning. A novel watermarking attack loss is introduced to break the MW systems. We empirically demonstrate that the WAN can successfully fool various block-based MW systems.

Index Terms—Watermarking attack, Multi-bit watermarking, Convolutional neural network (CNN), Watermark bit inversion

I. INTRODUCTION

DIGITAL watermarking is a technique used to protect copyright by embedding identification information, referred to as watermark, into the original image [1], [2]. Unlike visible watermarking, which inserts a watermark perceptible by the human visual system (HVS), invisible watermarking is an approach that embeds imperceptible watermarks. In particular, multi-bit watermarking (MW), which is a representative example of invisible watermarking, has been actively researched so that multi-bit information can be extracted from the watermarked image [3]. MW inserts watermarks by considering the fundamental requirements: *Imperceptibility*, which is the degree of invisibility of the watermarked signal, and *Robustness*, which is the ability of the watermark to survive against various watermarking attacks [4].

Imperceptibility is assessed using image quality assessment (IQA) metrics, which evaluate visual quality degradation caused by the watermark embedding. To assess robustness, a benchmark tool composed of various attacks, such as StirMark [5] and CheckMark [6], is applied to a watermarked image. These tools assess the robustness of the watermarking system by determining how well the inserted watermark can survive these simulated attacks. However, these tools attack watermarked images in a general way without considering the context of the watermarking system, so they cannot dig into the specific weak points of the watermarking system [7]. Moreover, these attacks degrade the visual quality beyond what is acceptable for commercial usage in the process of

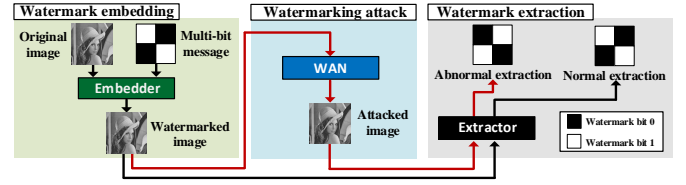


Fig. 1. How a watermarking attack network (WAN) works. The red arrow denotes the case in which a message deformed by WAN is extracted; our work can hinder the extraction of the watermark while maintaining visual quality, interfering with watermark extraction by deteriorating the image.

Instead, malicious users can design effective attacks to remove the watermark by targeting the MW and without visual degradation [7], which further deepens the gap between attacks in the real-world and existing benchmark tools. In this case, the designers of the watermarking system can assume a worst-case attack, where the watermark embedding and extraction algorithms are public (i.e., Kerckhoffs's principle [8]), to make systems more robust against adversaries. In this context, designing novel benchmark tools to create tests that are adequate for individual, specific watermarking systems to induce the false extraction of inserted information while maintaining a high quality level for the content is important.

Motivated by the need for a useful tool to model and understand the watermarking process, we propose a watermarking attack network (WAN) that exploits the weak points of individual watermarking systems without compromising visual quality. As illustrated in Fig. 1, the proposed WAN is devised to hinder the extraction of inserted watermarks by adding interference signals to mislead the watermarking extractor. With proposed loss function, our work can both induce abnormal extraction and generate a reconstructed image with a visual quality similar to the original content. We determine that the residual dense block-based architecture's ability to learn local and global features is suitable for analysing each MW method composed of various procedures and detailed attributes such as the watermarking domains and embedding algorithms [9]. The main contributions are listed as follows.

- To the best of our knowledge, this is the first attempt to successfully introduce a convolutional neural network (CNN)-based watermarking attack framework for interfering with the watermark extraction of MW systems.
- For specific MW methods, the WAN can apply subtle modification to induce the extraction of the watermark bit embedded in the image in an inverted state (e.g., $0 \rightarrow 1$ or $1 \rightarrow 0$). We experimentally demonstrate that our proposed WAN can successfully attack various watermarking systems [10]–[16] while conserving image quality.

II. BACKGROUND

A. Multi-bit Watermarking

Rather than using zero-bit watermarking to detect the presence or the absence of a watermark, MW can be used in var-

^{*} Seung-Hun Nam and Wonhyuk Ahn contributed equally to this work.

[†] Corresponding author: Seung-Hun Nam (e-mail: nam1202@kaist.ac.kr)

S.-H. Nam, W. Ahn, and I.-J. Yu are with the School of Computing, Korea Advanced Institute of Science and Technology (KAIST), Daejeon 34141, South Korea.

S.-M. Mun is with the Mobile Business, Samsung Electronics Co. Ltd., Suwon 443742, South Korea.

TABLE I
CATEGORIZATION OF MULTI-BIT WATERMARKING METHODS BASED ON
THE WATERMARKING DOMAINS AND EMBEDDING ALGORITHMS

Category	Attribute
Watermarking domain	Discrete cosine transform (DCT), discrete wavelet transform (DWT), nonsubsampling contourlet transform (NSCT), dual-tree complex wavelet transform (DTCWT), singular value decomposition (SVD), and QR decomposition (QRD)
Embedding algorithm	Spread spectrum (SS), improved spread spectrum (ISS), quantization (QT), and embedding for causing differences between sub-groups (DIF)

ious applications since the n -bit-long message ($\mathbf{m} = \{0, 1\}^n$) can be inserted in the host image I_o to get a watermarked image I_w . In particular, block-based MW systems [10]–[16], which insert a watermark bit (0 or 1) in each sub-block, are mainly used for multi-bit information insertion rather than the keypoint-based approach [3] due to the benefits that can be achieved by utilizing the entire domain. In detail, the transform domain such as DWT, DTCWT, DCT, NSCT, SVD, and QRD is first applied to each sub-block, and then watermark embedding is performed by applying an embedding algorithm such as SS, ISS, QT, and DIF to the selected domain (see Table I). In consideration of imperceptibility and robustness, MW methods select a watermarking domain and an embedding algorithm, and complex procedures such as perceptual masking [2] and template insertion [12] are added. In the extraction phase, message $\hat{\mathbf{m}}$ can be extracted from I_w in a blind fashion where the original image or any side information is not required. The performance of MW is evaluated in terms of imperceptibility and robustness. Specifically, the visual differences between I_o and I_w are determined using the IQA metrics, such as peak signal-to-noise ratio (PSNR) and structural similarity (SSIM), and robustness is evaluated by calculating bit error rate (BER) between \mathbf{m} and $\hat{\mathbf{m}}$.

B. Watermarking Attack and Motivation

Watermarking attacks are employed to evaluate the robustness of MW methods; let \tilde{I}_w be the attacked image of I_w . By comparing the messages extracted from I_w and \tilde{I}_w , a MW designer can evaluate the robustness of the MW by determining whether the hidden information survived [7]. Currently, StirMark [5] and CheckMark [6] are the representative benchmark tools that provide various types of common attacks such as signal processing operations and geometric distortions. As can be seen in Fig. 2, common watermarking attacks mounted in StirMark are accompanied by visual degradation and have a limitation of not being able to model the vulnerabilities of each MW method. That is, the more that a watermarking attack utilizes the characteristics of the targeted watermarking system, the more effective the attack is possible without image quality degradations.

With the development of neural networks, CNN-based MW methods [17] have been newly proposed, and they can be neutralised with adversarial attacks attempting to fool watermarking systems through malicious inputs; these are referred to as adversarial examples. However, attacking numerous handcrafted MW methods that contain non-differentiable operators with an adversarial attack is difficult. Although there is a differential evolution-based attack [18] that randomly modifies one pixel and query queries the extractor, it is difficult to

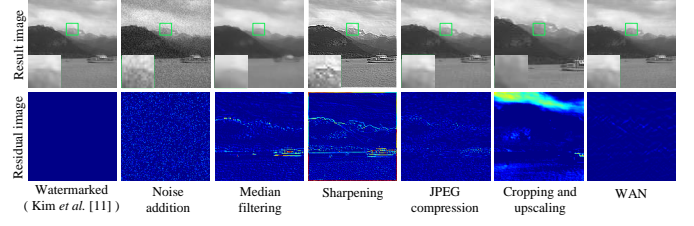


Fig. 2. Examples of the results of conducting watermarking attacks using StirMark and the proposed WAN. Examining the residual results between the original and attacked images shows that WAN achieves better visual quality than the simulated attack.

disable robust MW systems with only a few pixel changes. In addition, it is essential for a trained model to be able to attack numerous watermarked images generated from each MW method without additional training. To address these issues, we propose a CNN-based watermarking attack that automatically learns and exploits the weak points of individual watermarking systems.

III. WATERMARKING ATTACK NETWORK (WAN)

The proposed WAN targets block-based MW and needs one triple set of sub-block image patches, of I_o , watermarked images with bit 0 I_{w_0} , and watermarked images with bit 1 I_{w_1} , in the training phase. WAN takes I_{w_0} and I_{w_1} as inputs and reconstructs each of them into attacked images \tilde{I}_{w_0} and \tilde{I}_{w_1} , respectively. Our goal is to reconstruct images that mislead the watermarking extractor to decide on the wrong bit. In other words, when \tilde{I}_{w_0} and \tilde{I}_{w_1} are considered to have been inserted 1 bit and 0 bit, we judge the attack to be successfully done. On the other hand, the attacked image should be similar to the original to minimize visual degradation. We start with in-depth descriptions of loss functions consisting of watermarking attack loss and content loss and provide detailed descriptions of the architecture of the network and the mini-batch configuration.

A. Loss Function

The proposed WAN is trained to reconstruct attacked images containing an inverted watermark bit while minimizing the visual quality degradation. To achieve this, we propose a customized loss as an objective function to train the WAN as follows: $\mathcal{L} = \lambda_{wa}\mathcal{L}_{wa} + \lambda_c\mathcal{L}_c$, where \mathcal{L}_{wa} and \mathcal{L}_c represent watermarking attack loss, which is devised to change an inserted bit and content loss to minimize visual degradation, respectively. λ_{wa} and λ_c indicate predefined weight terms for each loss.

1) *Watermarking Attack Loss*: Existing watermarking methods vary in terms of the watermarking domains and embedding algorithms, so it is difficult to theoretically model MW in a single system. Moreover, conventional MW methods incorporate non-differentiable operations, so it is difficult for the neural network to learn directly from these methods even though step-by-step instructions are publicly available. We simplify this problem as the watermark signal is added to the original image in the pixel domain, and focus on the noise patterns that are decided by bit information. In other words, the residual signal arose by bit 0 insertion $R_{o,w_0} = |I_o - I_{w_0}|$ and the residual signal arisen by bit 1 insertion $R_{o,w_1} = |I_o - I_{w_1}|$,

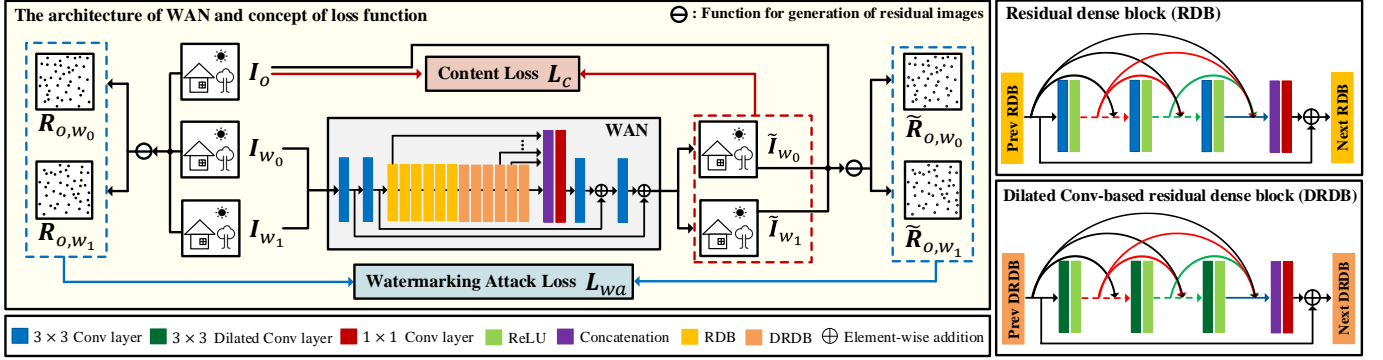


Fig. 3. Schematic illustration of the network architecture of our WAN framework.

which can be identified by neural networks. We hypothesise that the neural network can remove watermark signals in images and insert opposite noise patterns, which causes wrong bit extraction at the watermarking extractor. In this case, the attacked image \tilde{I}_{w_0} on I_{w_0} would have similar noise pattern $\tilde{R}_{o,w_0} = |I_o - \tilde{I}_{w_0}|$ to R_{o,w_1} , for which the one with bit 0 makes. The noise pattern \tilde{R}_{o,w_1} of the attacked image \tilde{I}_{w_1} on I_{w_1} would be similar to R_{o,w_0} , in the same way.

To capture the above observation, watermarking attack loss for the image of size $W \times H$, \mathcal{L}_{wa} is defined as follows: $\mathcal{L}_{wa} = \frac{1}{N} \sum_{i=1}^N |R_{o,w_0}^i - \tilde{R}_{o,w_1}^i| + \frac{1}{N} \sum_{i=1}^N |R_{o,w_1}^i - \tilde{R}_{o,w_0}^i|$, where superscript i refers to pixel location and $N = W \times H$. The first term of the equation is for deriving the watermark bit 1 inserted in I_{w_1} into 0, and the second term is for deriving bit 0 inserted in I_{w_0} into bit 1. As depicted in Fig. 3, a loss is designed by pairing the residual images before and after going through the WAN according to the inserted bit and reducing the difference between the paired images. Through the \mathcal{L}_{wa} , it is possible to add a fine noise-like attack that inverts the actually inserted bit during the process of passing the watermarked images over the WAN.

2) *Content Loss*: It is important to preserve visual quality while adding adversarial signals. To this end, content loss is adopted to reduce the visual differences between the original content I_o and its corresponding reconstructed images, including \tilde{I}_{w_0} and \tilde{I}_{w_1} attacked by the WAN (see Fig. 3). Inspired by the papers [19] demonstrating that ℓ_1 loss can bring better visual quality than ℓ_2 loss for general restoration tasks, the content loss of \mathcal{L}_c is defined as follows: $\mathcal{L}_c = \frac{1}{N} \sum_{i=1}^N \sum_{j=0}^1 |I_o^i - \tilde{I}_{w_j}^i|$. From \mathcal{L}_c , it is possible to conduct a watermarking attack while minimizing visual quality degradations in the original content. Through the final objective function of \mathcal{L} combined with \mathcal{L}_c and \mathcal{L}_{wa} , the proposed WAN can reconstruct images in a way that adversely affects the extraction of the inserted bit while maintaining the inherent properties of the original content.

B. Model Architecture

Fig. 3 illustrates the neural network architecture for our model. We follow the network design from the residual dense network (RDN) [9] that is used for the learning of the local and global features and the ability of image restoration. The residual dense block (RDB) constituting the RDN is composed of densely connected convolutional (Conv) layers and is specialized in extracting abundant local features. In addition, a

dilated Conv-based dense block (DRDB) with a dilated Conv layer applied to the RDB is utilized, and the DRDB is placed in the deeper layer to increase the receptive field. In the proposed WAN, the pooling layer and up-sampling are excluded, so the input and output sizes are the same ($\{I_{w_0}, I_{w_1}, \tilde{I}_{w_0}, \tilde{I}_{w_1}\} \in \mathbb{Z}^{1 \times W \times H}$). The first and second Conv layers are placed to extract shallow features and conduct global residual learning. Next, by placing RDBs in a shallow layer and subsequent DRDBs in a deeper layer, the local features is learned, and the receptive field increased as the layer deepened. We expect sub-components for local residual learning and local feature fusion commonly used in RDB and DRDB to help our model learn low-level features caused by watermark embedding. After that, by the concatenation layer followed by 1×1 and 3×3 Conv layers, dense local features extracted from the set of RDBs and DRDBs are fused in a global way. The deep part of the proposed WAN is composed for global residual learning based on shallow feature maps.

C. Mini-batch Configuration

Since invisible MW is the approach of inserting a watermark so that it is unnoticeable by HVS, mini-batch configuration suitable for fine signal learning is required instead of the standard mini-batch used in high-level computer vision. The authors in [20] presented paired mini-batch training, which is efficient for learning low-level features such as multimedia forensics and steganalysis. To aid in learning the discriminative features between watermarked results more effectively, paired mini-batch training is employed. That is, I_{w_0} and I_{w_1} generated for the same original image I_o are allocated in a single batch, which allows the proposed WAN to learn fine signals due to the differences in the fine signals caused by the watermark bit. In detail, when the batch size is b_s , $\frac{b_s}{2} I_{w_0}$ images are selected first, and then $\frac{b_s}{2} I_{w_1}$ images corresponding to I_{w_0} are assigned to be in the same batch. The entire dataset is shuffled every epoch.

IV. EXPERIMENTS

A. Datasets

BOSSbase [21] and BOWS [22] datasets are used to generate 20,000 original grey-scale images with a size of 512×512 . We resize them to 64×64 (i.e., $W = H = 64$) using the default settings in MATLAB R2018a, the resized images are divided into three sets for training, validation, and test (with a 14 : 1 : 5 ratio). The block-based MW methods [10]–[16]

TABLE II
QUALITATIVE EVALUATION RESULTS OF THE PROPOSED WAN ON THE TEST SET WITH ONE BIT AND FOUR BITS OF WATERMARK CAPACITY

Multi-bit watermarking system				1 bit of watermark capacity						4 bits of watermark capacity					
				Non-attack			WAN			Non-attack			WAN		
Method	WD	EA	SD	PSNR	SSIM	BER	PSNR	SSIM	BER	PSNR	SSIM	BER	PSNR	SSIM	BER
Kim [12]	DCT	SS	1×64	35.55	0.938	0.026	34.04	0.956	0.893	35.53	0.938	0.049	34.79	0.963	0.905
Lin [10]	DCT	ISS	8×8	36.36	0.973	0	32.96	0.961	1.000	37.54	0.974	0	33.77	0.966	0.999
Lin [10]	DCT	ISS	16×16	41.86	0.988	0	37.47	0.979	0.996	42.62	0.987	0	37.44	0.980	0.993
Parah [14]	DCT	DIF	8×8	36.43	0.945	0	38.62	0.980	0.848	36.41	0.928	0	39.82	0.987	0.752
Su [15]	QR	DIF	8×8	36.59	0.974	0	33.05	0.96	1.000	37.55	0.973	0	33.64	0.962	0.998
Makbol [13]	DWT, SVD	DIF	8×8	38.98	0.986	0.002	37.70	0.985	0.988	39.71	0.985	0.002	38.09	0.985	0.990
Makbol [13]	DWT, SVD	DIF	16×16	40.59	0.986	0.001	38.79	0.986	0.985	40.68	0.981	0.001	38.51	0.981	0.987
Kim [11]	DTCWT	QT	-	36.61	0.972	0.021	35.52	0.972	0.622	37.52	0.973	0.044	35.85	0.975	0.681
Nam [16]	NSCT	QT	-	39.21	0.987	0.013	36.54	0.980	0.946	40.64	0.987	0.041	37.22	0.982	0.885
Average	-	-	-	38.02	0.972	0.007	36.08	0.973	0.920	38.69	0.970	0.015	36.57	0.976	0.910

* Notes: WD, EA, and SD represent abbreviation of the watermarking domain, the embedding algorithm, and the size of subdivision, respectively.

are used to generate watermarked images, and the images are generated by embedding watermark bits (0 or 1) into the original images given for each method listed in Table II. These methods perform watermark bit extraction in blind fashion. The detailed parameters for the watermark embedding and extraction of each MW method will be provided online later. For further quantitative and qualitative evaluation, we additionally generate test images sized 128×128 for the test set. Watermarked images with resolutions of 128×128 have a watermark capacity of 4 bits. In the experiment, the WAN-based attacks and watermark bit extraction proceeds for each 64×64 patch.

B. Implementation Details and Training Settings

The number of RDB, DRDB, Conv layer per RDB and DRDB, feature-maps, and the growth rate are set to 6, 6, 6, 32, and 16, respectively. For the 3×3 dilated Conv layer, we use dilation set to 1 and set the padding and stride to 2. We build our network using PyTorch and run the experiments on NVIDIA GeForce GTX 1080 Ti. In the experiments, we use the Adam optimizer with a learning rate of 10^{-4} and momentum coefficients $\beta_1 = 0.9$, $\beta_2 = 0.999$. The size of mini-batch b_s is set to 32, and each mini-batch is configured for paired mini-batch training [20]. The proposed WAN is trained with the hyperparameters $\lambda_c = 0.4$ and $\lambda_{wa} = 0.3$ during 30 epochs, and the best model is selected as the one that maximizes BER on the validation set for each MW method.

C. Quantitative Evaluation

First, a quantitative evaluation of the WAN is conducted in terms of watermark extraction interference and the visual quality of attacked images. We use IQA metrics, PSNR (dB) and SSIM, to determine the imperceptibility and BER to evaluate attacks to get quantitative results. The middle part of Table II shows the performance results of our work on the test set with 1 bit capacity generated through each MW method, which are composed of various attributes. In non-attack situations, each method has a low BER value of 0.026 or less, while the average BER value increases dramatically to 0.920 after WAN is applied. In particular, for MW methods in [10], [13], [15], the BER value of methods rise to 0.985 or more, which means that the WAN has learned a fine signal generated during the watermark embedding and successfully performs bit inversion. For [14] and [11], they have lower BER values of 0.848 and 0.622, respectively, and we expect this to be an issue because these robust MW methods are

composed of sophisticated operations that are hard to model and attack through the WAN. In general, making the extraction performance at a random guessing level is considered a very fatal attack, and it is validated that the proposed \mathcal{L}_{wa} successfully leads to abnormal extraction of watermark bits.

In addition, minimizing the visual damage caused by watermarking attacks is an important issue in our work. To do this, we introduce \mathcal{L}_c , and the gain of visual quality obtained from the loss can be analyzed through PSNR and SSIM values with I_o in Table II. The average PSNR and SSIM values in non-attack situation are 38.02 dB and 0.972, respectively. After the WAN is applied, average PSNR decreases by 1.94 dB, and SSIM remained similar to that before the attack. The simulated attacks in [5], [6] are not designed considering the visual property of content, so it is accompanied by visual degradation during the attack process. Meanwhile, our model based on \mathcal{L}_c is capable of inducing the drastic reversal of the watermark bit with acceptable small loss of image quality.

We further conduct the experiments by applying the trained WAN model with stride 64 to a test set with 4 bits of watermark capacity. As listed on the right side of Table II, the average PSNR, SSIM, and BER values for the attacked images over the WAN are 36.57 dB, 0.976, and 0.910, respectively. Compared with the results for 1 bit capacity, we can confirm that the WAN's overall performance is maintained even when the watermark capacity is increased. For some MW methods [11], [14], there is an improvement and degradation in performance, which is presumed to be caused by the dependence of each MW on the inherent texture and content characteristics of given images. Overall, the results of quantitative evaluation show that the proposed WAN is suitable for testing MW methods as a benchmark tool in terms of interference of watermark extraction, maintenance of visual quality, and scalability according to watermark capacity.

D. Qualitative Evaluation

Next, we performed qualitative evaluation in terms of visual quality. Fig. 4 shows the examples of the watermarked image with 4 bit of capacity and the attacked image of the proposed WAN. As shown in the top row of Fig. 4, the types of low-level distortion caused by watermark embedding vary by MW method while having similar high-level features (i.e., inherent content of I_o). The proposed WAN with \mathcal{L}_{wa} and \mathcal{L}_c can hinder watermark extraction by learning these fine feature and induces the attacked image to visually follow the original

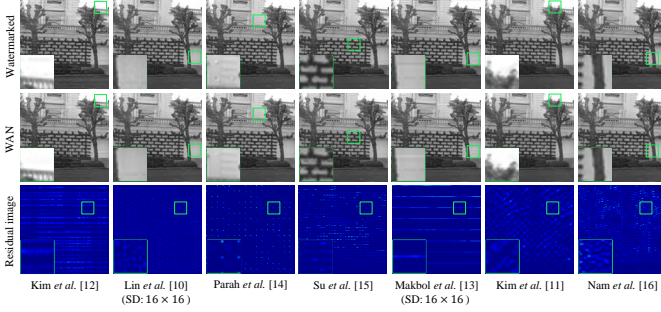


Fig. 4. Examples of attacked images generated from the WAN applied to MW methods. For visualization, the residual images were multiplied by a factor of 3.



Fig. 5. Comparison of visual quality of the WAN and numerous attacks in StirMark.

content. Our work can produce natural attacked results that very similar to images in non-attack situations (see second row of Fig. 4). Furthermore, we observe that the residual images in the bottom row of the figure have different patterns depending on the method. From this, we can confirm that WAN, when trained to learn the properties (e.g., the watermarking domain and embedding method) of each MW, attacks watermarked images adaptively.

Fig. 5 compares results of the our model and StirMark [5] consisting signal processing operations and geometric distortions. For fairness in comparison, attacked images generated through attack parameters of StirMark that cause random guessing of bit extraction (e.g., BER = 0.5) are compared. As mentioned above, the StirMark is not an approach of attacking by modeling the vulnerability of the MW method or considering inherent content, so it is accompanied by unwanted visual degradation in the attack process (see magnified sub-figures in Fig. 5). In contrast, our WAN can adversely affect the extraction of the inserted bit while maintaining the inherent properties of the original content. From the results of qualitative evaluation, it is confirmed that the CNN architecture specialized for image restoration and the proposed loss function are effective in generating natural attacked images.

V. CONCLUSION

In this paper, we propose a novel CNN-based benchmark tool for block-based MW methods that learns the weak points of the targeted watermarking approach and attacks watermarked images to mislead the watermarking extractor with minimal visual degradation. To achieve this goal, we design customized losses of a watermarking attack loss for abnormal bit extraction and a content loss to maintain visual quality. Through quantitative and qualitative experiments with a vari-

ety of MW methods, we demonstrate that the proposed WAN performs more effective attacks than existing benchmark tools in terms of maintaining visual quality and interfering with watermark extraction. We expect that the proposed WAN will be helpful for watermarking designers to test the robustness of their MW methods.

REFERENCES

- [1] I. Cox, M. Miller, J. Bloom, J. Fridrich, and T. Kalker, *Digital watermarking and steganography*. Morgan kaufmann, 2007.
- [2] M. Barni, F. Bartolini, V. Cappellini, and A. Piva, "A dct-domain system for robust image watermarking," *Signal processing*, vol. 66, no. 3, pp. 357–372, 1998.
- [3] S.-H. Nam, W.-H. Kim, S.-M. Mun, J.-U. Hou, S. Choi, and H.-K. Lee, "A sift features based blind watermarking for dibr 3d images," *Multimedia Tools and Applications*, pp. 1–40, 2017.
- [4] I. J. Cox, J. Kilian, F. T. Leighton, and T. Shamon, "Secure spread spectrum watermarking for multimedia," *IEEE transactions on image processing*, vol. 6, no. 12, pp. 1673–1687, 1997.
- [5] F. A. Petitcolas, R. J. Anderson, and M. G. Kuhn, "Attacks on copyright marking systems," in *International workshop on information hiding*. Springer, 1998, pp. 218–238.
- [6] S. Pereira, S. Voloshynovskiy, M. Madueno, S. Marchand-Maillet, and T. Pun, "Second generation benchmarking and application oriented evaluation," in *International workshop on information hiding*. Springer, 2001, pp. 340–353.
- [7] S. Voloshynovskiy, S. Pereira, V. Iquise, and T. Pun, "Attack modelling: towards a second generation watermarking benchmark," *Signal processing*, vol. 81, no. 6, pp. 1177–1214, 2001.
- [8] A. Kerckhoffs, *La cryptographie militaire, ou, Des chiffres usités en temps de guerre: avec un nouveau procédé de déchiffrement applicable aux systèmes à double clef*. Librairie militaire de L. Baudoin, 1883.
- [9] Y. Zhang, Y. Tian, Y. Kong, B. Zhong, and Y. Fu, "Residual dense network for image super-resolution," in *Proceedings of the IEEE conference on computer vision and pattern recognition*, 2018, pp. 2472–2481.
- [10] Y.-H. Lin and J.-L. Wu, "A digital blind watermarking for depth-image-based rendering 3d images," *Broadcasting, IEEE Transactions on*, vol. 57, no. 2, pp. 602–611, June 2011.
- [11] H.-D. Kim, J.-W. Lee, T.-W. Oh, and H.-K. Lee, "Robust dt-cwt watermarking for dibr 3d images," *Broadcasting, IEEE Transactions on*, vol. 58, no. 4, pp. 533–543, Dec 2012.
- [12] W.-H. Kim, J.-U. Hou, H.-U. Jang, and H.-K. Lee, "Robust template-based watermarking for dibr 3d images," *Applied Sciences*, vol. 8, no. 6, 2018. [Online]. Available: <http://www.mdpi.com/2076-3417/8/6/911>
- [13] N. M. Makbol, B. E. Khoo, and T. H. Rassem, "Block-based discrete wavelet transform-singular value decomposition image watermarking scheme using human visual system characteristics," *IET Image Processing*, vol. 10, no. 1, pp. 34–52, 2016.
- [14] S. A. Parah, J. A. Sheikh, N. A. Loan, and G. M. Bhat, "Robust and blind watermarking technique in dct domain using inter-block coefficient differencing," *Digital Signal Processing*, vol. 53, pp. 11–24, 2016.
- [15] Q. Su, G. Wang, X. Zhang, G. Lv, and B. Chen, "An improved color image watermarking algorithm based on qr decomposition," *Multimedia Tools and Applications*, vol. 76, no. 1, pp. 707–729, 2017.
- [16] S.-H. Nam, S.-M. Mun, W. Ahn, D. Kim, I.-J. Yu, W.-H. Kim, and H.-K. Lee, "Nsct-based robust and perceptual watermarking for dibr 3d images," *IEEE Access*, vol. 8, pp. 93 760–93 781, 2020.
- [17] S.-M. Mun, S.-H. Nam, H. Jang, D. Kim, and H.-K. Lee, "Finding robust domain from attacks: A learning framework for blind watermarking," *Neurocomputing*, vol. 337, pp. 191–202, 2019.
- [18] J. Su, D. V. Vargas, and K. Sakurai, "One pixel attack for fooling deep neural networks," *IEEE Transactions on Evolutionary Computation*, vol. 23, no. 5, pp. 828–841, 2019.
- [19] H. Zhao, O. Gallo, I. Frosio, and J. Kautz, "Loss functions for image restoration with neural networks," *IEEE Transactions on computational imaging*, vol. 3, no. 1, pp. 47–57, 2016.
- [20] J.-S. Park, H.-G. Kim, D.-G. Kim, I.-J. Yu, and H.-K. Lee, "Paired mini-batch training: A new deep network training for image forensics and steganalysis," *Signal Processing: Image Communication*, vol. 67, pp. 132–139, 2018.
- [21] P. Bas, T. Filler, and T. Pevný, "Break our steganographic system: the ins and outs of organizing boss," in *International workshop on information hiding*. Springer, 2011, pp. 59–70.
- [22] P. Bas and T. Furon, "Bows-2," 2007.